



King's Research Portal

DOI:

[10.1161/CIRCULATIONAHA.111.056952](https://doi.org/10.1161/CIRCULATIONAHA.111.056952)

Document Version

Peer reviewed version

[Link to publication record in King's Research Portal](#)

Citation for published version (APA):

Barallobre-Barreiro, J., Didangelos, A., Schoendube, F. A., Drozdov, I., Yin, X., Fernandez-Caggiano, M., ... Mayr, M. (2012). Proteomics Analysis of Cardiac Extracellular Matrix Remodeling in a Porcine Model of Ischemia/Reperfusion Injury. DOI: 10.1161/CIRCULATIONAHA.111.056952

Citing this paper

Please note that where the full-text provided on King's Research Portal is the Author Accepted Manuscript or Post-Print version this may differ from the final Published version. If citing, it is advised that you check and use the publisher's definitive version for pagination, volume/issue, and date of publication details. And where the final published version is provided on the Research Portal, if citing you are again advised to check the publisher's website for any subsequent corrections.

General rights

Copyright and moral rights for the publications made accessible in the Research Portal are retained by the authors and/or other copyright owners and it is a condition of accessing publications that users recognize and abide by the legal requirements associated with these rights.

- Users may download and print one copy of any publication from the Research Portal for the purpose of private study or research.
- You may not further distribute the material or use it for any profit-making activity or commercial gain
- You may freely distribute the URL identifying the publication in the Research Portal

Take down policy

If you believe that this document breaches copyright please contact librarypure@kcl.ac.uk providing details, and we will remove access to the work immediately and investigate your claim.

Proteomics of the epicardial fat secretome and its role in postoperative atrial fibrillation

Alessandro Viviano, MD MRCS,¹ Xiaoke Yin, PhD,² Anna Zampetaki, PhD,² Marika Fava, Mark Gallagher, MD, PhD,¹ Manuel Mayr, PhD,² Marjan Jahangiri, FRCS¹

1. Department of Cardiothoracic Surgery, St. George's Hospital, University of London, UK
2. King's British Heart Foundation Centre, King's College, London, UK

Address for correspondence:

Marjan Jahangiri, FRCS (CTh),
Department of Cardiac Surgery,
St. George's Hospital,
Blackshaw Road,
London SW17 0QT,
United Kingdom
Tel: +44-2087253565, Fax: +44-2087252049
Email: marjan.jahangiri@stgeorges.nhs.uk

Word count: 5169

Sources of Funding: This study was funded by St. George's Charitable Foundation.

Conflict of interest: none declared.

Condensed abstract

Systemic inflammatory response to cardiac surgery is a known trigger for postoperative atrial fibrillation. Latent predisposing factors may reside at the protein level. Proteins released by the epicardial adipose tissue preceding the development of postoperative atrial fibrillation were examined in order to explore possible mechanistic links in its pathogenesis.

What's New

- We present the first proteomics study to describe the EAT secretome
- We characterised EAT proteins as a possible substrate for the development of POAF
- Various proteins were differentially expressed in the EAT secretome in patient who later developed POAF
- Amongst those gelsolin, involved in inflammation and ion channel regulation, was associated with the maintenance of sinus rhythm.
- Understanding the role of EAT may offer novel insights into prevention and treatment of AF.

Introduction

Atrial fibrillation (AF) is the most common postoperative arrhythmia following cardiac surgery affecting more than one third of patients and is associated with increased morbidity and mortality, prolonged hospitalisation, and increased costs.¹ The genesis of postoperative AF (POAF) is multifactorial including predisposing factors and acute triggering events such as operative trauma and myocardial ischaemia, electrolyte imbalances, inflammation and oxidative stress.

Epicardial Adipose Tissue (EAT) is a type of specialised visceral fat distributed mainly around the atrioventricular and interventricular grooves and along the coronary arteries; smaller amount is also seen on the atrial appendages

Hatem and colleagues highlight how the abundance of EAT is associated with AF. They suggest EAT could exert a paracrine activity onto the myocardium by producing a large variety of bioactive substances (adipokines) with both proinflammatory and antiinflammatory properties.² Furthermore infiltrates of EAT are seen deep in the myocardium which could trigger arrhythmias by altering propagation of the depolarizing wave, and via remodelling of the atrial myocardium.³

To date, the relationship between EAT proteome and the development of POAF has not been investigated.

Salgado-Somoza et al conducted to date the only proteomic study of the EAT. They compared EAT and subcutaneous adipose tissue (SAT) in patients undergoing heart surgery with 2D-DIGE and mass spectrometry. They found that proteins related to oxidative stress appeared to be more expressed in EAT rather than SAT in patients with coronary artery disease. They conclude that EAT is exposed to greater oxidative stress compared to SAT in patients with cardiovascular disease suggesting its possible association with myocardial stress.⁴

The proteome is the determinant of the cell phenotype and its variations are translated into changes in the cell and tissue functions. Unlike the genome, the proteome is much closer to the disease phenotype and can better elucidate the processes behind the manifestation and progression of disease. Proteomics investigates the proteome via different advanced techniques such as two-dimensional difference in-gel electrophoresis (2D-DIGE) and high performance liquid chromatography-tandem mass spectrometry (HPLC-MS/MS). Our aim was to evaluate the EAT secretome and investigate substrate changes that precede AF and that may contribute to its genesis following cardiac surgery.

Methods

Patients

EAT samples were collected from 76 consecutive patients, 50 for proteomic analysis and 26 for gene expression studies. All patients were undergoing first time isolated coronary artery bypass graft surgery (CABG) with no history of AF, no antiarrhythmic therapy other than beta blockers and no immunomodulating therapy. Standardised anaesthetic, perfusion, and surgical protocols were followed. All patients underwent on-pump CABG at 35C. All patients received beta blockers on the first post-operative day, unless contraindicated due to allergy, severe bradycardia or hypotension. No other specific therapy was adopted for prevention of POAF. Routine postoperative heart rhythm assessment was achieved with continuous telemonitoring for 48 hours after surgery and 3-hourly clinical examinations thereafter. Twelve-lead electrocardiograms were also assessed on day 0, 2 and 4 after surgery. Amiodarone, intravenous or oral after appropriate loading, was the treatment of choice in patients who developed AF.

Statistical Analysis

Statistical analyses were performed using Prism version 6.0 and Microsoft Excel 2013 software. The unpaired Student's t-test was used to assess statistical significance between normally distributed data; nominal variables were compared using the Fisher's exact test of independence. Statistical difference was indicated by a P value of <0.05. Data are expressed as mean \pm SEM or mean \pm STDEV as specified.

Tissue Sampling and Preparation

EAT tissue was obtained before establishing cardiopulmonary bypass (CPB) in order to avoid confounding factors generated by the exposure of blood to foreign material, in particular the initiation of inflammatory response of CPB. Approximately 500 mg of EAT was harvested, most commonly from the right ventricle. Samples for proteomic analysis of the secretome were finely minced and immediately incubated in 1-2 ml of high glucose serum free condition medium (DMEM, High Glucose, GlutaMAX™, Invitrogen), depending on sample size, enriched with insulin (Insulin human - recombinant, expressed in yeast, Sigma I2643) for 24 hours at 37° C and controlled 5% CO₂ in order to stimulate adipokine production by the adipocyte and secretome release. Condition medium was utilised for 2D-DIGE of the secretome whereas the remaining fat tissue was subsequently used for protein extraction and western blot validations.

26 samples were stored in RNA extraction solution (Quiazol, Qiagen), two were later discarded as not suitable for analysis, the remaining 24 were subsequently analysed for gene expression.

EAT protein extraction: RIPA buffer (RadioImmuno Precipitation Assay buffer, ab156034, MitoSciences, abcam) supplemented with protease inhibitors was used to extract proteins

from approximately 100 mg of EAT. Protein concentration was determined by RC DCTM, Bio-Rad.

Two-dimensional difference in-gel electrophoresis (2D-DIGE): 10 vs. 10 protein samples from each group were analysed. Prior to proteomic analysis, samples were purified using a commercial cleanup kit (ReadyPrep™ 2-D Cleanup Kit Bio Rad), urea and non-ionic detergents were used to unfold proteins and protease inhibitors were added. Proteins were then resuspended in DIGE lysis buffer (8M urea, 4% w/v CHAPS, 30 mM TrisCl, pH 8.5). Protein concentration was measured with Bradford assay methodology (Bio-Rad).

After clean-up, proteins were redissolved in DIGE lysis buffer (8M urea, 4% w/v CHAPS, 30mM Tris-HCl, pH 8.5).

Randomised labeling was applied. 50µg proteins per each sample from a given pair (i.e. POAF and SR group) were randomly labelled with Cy3 or Cy5 fluorescent dye (CyDye, GE Healthcare). Additionally a pooled internal standard was created by mixing the same amount of all samples and labelled with Cy2. Paired samples and internal standard (biological replicate) were run on every gel effectively creating a technical replicate to normalize against, enabling to distinguish biological “real” variation from technical variation.

After protein labelling the same protein amount of two different paired samples and internal standard, were mixed. 2x DIGE buffer (8M urea, 4% w/v CHAPS, 2% w/v DTT, 2% v/v Pharmalyte pH 3-10) and rehydration buffer (8M urea, 0.5% w/v CHAPS, 0.2% w/v DTT, 0.2% w/v Pharmalyte pH 3-10 and trace Bromophenol blue) were added to the mixed sample to a final volume of 450 µl. The samples were loaded on IPG strips (18cm, pH 3-10 nonlinear, GE healthcare). The isoelectric focusing (IEF) was carried out at 0.05mA/strip for 28 kWh at 20°C after overnight rehydration. For the second dimension large format 12% Tris-Glycine gels were casted, IPG strips placed on top of the gels and sodium dodecylsulphate

polyacrylamide gel electrophoresis (SDS-PAGE) was run at 16W/gel until blue dye front had migrated off the end of the gel. Subsequently protein spots were visualized by fluorescence scanner (Ettan DIGE Imager, GE health care).

Silver staining (PlusOne silver staining kit, GE healthcare) of the gels allowed later visualisation of the corresponding protein spots for manual spot picking. In order to analyse differentially expressed proteins in the two sample groups, specialised software was used (DeCyder 7.0, GE Healthcare). A pick list of differentially expressed proteins ($p < 0.05$, ratio ≥ 1.2 or ratio ≤ -1.2) was generated and spots manually picked.

Liquid Chromatography Tandem Mass spectrometry (LC-MS/MS): In-gel digestion with trypsin was performed according to published methods modified for use with an Investigator ProGest (Digilab) robotic digestion system.⁵ After tryptic digestion, peptides were separated on a reverse-phase nanoflow HPLC system (Dionex UltiMate 3000 RSLCnano). The column (Acclaim PepMap100, 75 μm x 25 cm, 3 μm , 100Å, Thermo Fisher Scientific) was coupled to a nano spray source (Picoview) directly connected to LTQ Orbitrap XL mass spectrometer (Thermo Fisher Scientific). Spectra were collected using full MS scan mode with orbitrap over the mass-to-charge (m/z) range 350–1600 followed by 6 data-dependent MS2 scan. Extract_msn.exe was used to generate MS/MS peak lists that were matched to a human database (UniProtKB/Swiss-Prot Release 2013_08, 20,267 protein entries) using Mascot 2.3.01 (Matrix science). The following parameters were used: parent mass tolerance 10ppm, fragment mass tolerance 0.8Da, carbamidomethylation on cysteine as fixed modification and oxidation on methionine as variable modification, 2 missed cleavages were allowed. Scaffold (version 4.3.2, Proteome Software Inc.) was used to validate MS/MS-based peptide and protein identifications. Peptide identifications were accepted if they could be established at greater than 95.0% probability as specified by the Peptide Prophet algorithm. Protein

identifications were accepted if they could be established at greater than 99.0% probability and with at least 2 peptides.

Western blotting: validations were performed by western blotting on 6 vs. 6 EAT protein extracts samples. 12 µg of proteins were loaded with sample buffer and separated on Bis-Tris 4% to 12% polyacrylamide gradient gels (NuPage, Life-Technologies) using SDS running buffer (NuPAGE Mops SDS Running Buffer, Invitrogen) at 130V constant voltage. The gel was sandwiched with a nitrocellulose blotting membrane (GE healthcare life sciences) and proteins transferred to it applying a constant electrical current at 350mA in transfer buffer (Tris Base 25 mM, Glycine 200mM, 20% methanol) for 2.5 hours. Membranes were blocked in 5% milk-PBST, probed overnight at 4°C with anti-gelsolin antibody (1:1000, rabbit polyclonal, ab74420, abcam) and subsequently incubated in species-specific secondary antibodies (Dako). Enhanced chemiluminescence (ECL; GE Healthcare) was applied to the membranes and X-ray films exposed into cassettes. Films were developed using Kodak automated x-ray film developer.

RNA extraction: 26 samples were prepared for qPCR. Total RNA was isolated from samples weighing 80 to 150 mg previously stored in 700 µl of QIAzol Lysis Reagent using miRNeasy Mini Kit (QIAGEN®) as per manufacturer's instructions. Total recovered RNA was eluted in 25 µl of nuclease free H₂O. RNA concentration and purity were evaluated by using NanoDrop 1000 spectrophotometer (Thermo Fisher Scientific). In two samples RNA quality was found to be suboptimal, the remaining 24 samples were later utilised for analysis.

Reverse transcription (RT): 400 ng of RNA were reversed transcribed into cDNA using the High Capacity Reverse Transcriptase kit (Life Technologies) according to manufacturer

instructions. RT-PCR reaction program was set as follows: samples were initially denatured at 25°C for 5 minutes, then reverse transcribed for 90 minutes at 42°C, and finally the reverse transcriptase enzyme was inactivated for 15 minutes at 72°C. Samples were then diluted to 10ng/μl using RNase free water.

qPCR: gene expression study was performed via qPCR using TaqMan assay for gelsolin gene (Life technologies Hs00609272_m1). SP1 (Specificity Protein 1) was used as a normalization control. The PCR plate was loaded with 2.25 μl of RT product and qPCR was performed on Viia7 system thermocycler (Thermo Fisher Scientific). Programme was set at 50°C for 2 min, 95°C for 10 min, followed by 40 cycles of 95°C for 15 sec and 60°C for 1 min.

The study was commenced following approval from the Regional Ethical Committee (REC number 12/LO/0422) and institutional Research and Development office. All patients gave written informed consent.

Results

Patients were divided in two groups according to the development of POAF.

From the proteomics group of 50 patients, 16 developed POAF and 34 remained in SR. Out of those 10 vs. 10 were appropriately matched for age, sex, medications (in particular matching them for beta-blockers), cardiovascular risk profile and intraoperative variables (number of grafts, cross clamp and cardiopulmonary bypass time) and utilised for 2D-DIGE analysis. Furthermore, equally matched 6 vs. 6 were later utilised for Western Blot validation analysis.

From the gene expression group of 26 patients, 8 developed POAF and 18 remained in SR.

Two samples were later discarded as RNA deteriorated. All remaining samples (16 vs. 8) were then utilised for qPCR analysis.

Proteomics

For the proteomics study, we analysed 10 vs. 10 EAT secretome samples (Table 1). After 2D-DIGE analysis of the EAT secretome, a total of 35 spots were identified (Figure 1), corresponding to 26 differentially expressed proteins (Table 2). Six proteins were found to be significantly upregulated in the POAF group. All remaining proteins were downregulated.

Several proteins of interest, in particular related to inflammation and oxidative stress were differentially expressed in the proteomics analysis.

Amongst those gelsolin was significantly downregulated in the POAF group ($p=0.031$).

A protein spot containing selenium binding protein-1 (SBP-1) was differentially expressed in the EAT, being upregulated in patients who developed POAF ($p = 0.049$). Dimethylarginine dimethylaminohydrolase 2 (DDAH2) was also differentially expressed in the EAT, being increased in the POAF group ($p = 0.04$). A protein spot containing catalase was differentially expressed in the EAT secretome, being increased in the POAF group ($p = 0.004$).

Western blotting

Western blot validation of findings was performed on 6 vs. 6 EAT protein extracts. As a loading control a silver stain of a gel containing all selected samples was performed to ensure equal amount of proteins was loaded. Western blot analysis of the tissue extracts confirmed a significant reduction in gelsolin in the AF group ($p<0.001$) as shown in Figure 2. Validations for the remaining targets did not show statistically significant differences.

qPCR

Gene expression studies were performed via qPCR on 16 vs. 8 samples, controls and POAF respectively (Table 3). Gene expression for gelsolin was significantly reduced in the AF

group ($p=0.038$), confirming the proteomics findings (Figure 3). Gene expression for the remaining targets did not show statistically significant variations.

Discussion

The pathogenesis of AF is multifactorial and the mechanisms of it are not yet fully elucidated. Iwasaki and colleagues describe the important interaction between initiating triggers, such as rapidly firing ectopic in the pulmonary veins and abnormal atrial substrates.⁶ This can be translated in the postoperative setting as a synergistic interaction between surgery-induced triggering factors and pre-existing abnormal atrial substrates reaching the 'AF threshold'. In the apparently normal heart, predisposing factors may be subtler.

Aim of our study was to explore the pre-existing activity of the EAT by analyzing the secretome which could act as substrate in the myocardial environment possibly modulating the susceptibility to POAF.

Systemic inflammatory response to cardiac surgery and oxidative stress are important factors implicated in the development of POAF.⁷⁻⁸ Gelsolin exerts antiinflammatory properties by severing actin filaments. DDAH2 degrades nitric oxide synthase inhibitor ADMA (asymmetric dimethylarginine), known to increase oxidative stress. SBP-1 and catalase also have anti-oxidant properties.

Amongst the array of differentially expressed proteins, we believe gelsolin highlights possible interesting links between EAT and AF.

Gelsolin was shown to be downregulated in the POAF group by three independent techniques: in the EAT secretome by 2D-DIGE and LC-MS/MS, on the EAT protein extracts by Western blot, and at the gene level by qPCR.

2D-DIGE methodology may reveal changes in protein net expression, as demonstrated for gelsolin (consistent changes in 2D gels, Western blot and gene expression), or changes in

post-translational modifications, which may not be possible to validate by Western blot analysis or gene expression studies. These modifications in fact are generally enzymatic covalent addition of functional groups to the protein or cleavage of regulatory subunits taking place during or after protein biosynthesis, which increase the functional diversity of the proteome.

Inflammation and ion channel regulation: the role of gelsolin

Anti-inflammatory adipokines secreted by the epicardial fat such as adiponectin have shown protective effect against AF following cardiac surgery.² Lymphomononuclear infiltrates and fibrosis have also been described in histological sections of atrial tissue of patients with AF.⁹ Associations between inflammatory markers such as CRP and interleukin 6 (IL-6) and AF have been proposed.¹⁰⁻¹¹

Ion channel function is involved in the genesis of POAF and in particular the influx of Ca^{2+} through the L-type Ca^{2+} channels, the main current generating the plateau phase of the atrial action potential. Van Wagoner et al. described how the L-Type Calcium Current (I_{CaL}) in atrial myocytes is increased in patients developing postoperative AF. Triggered activity (e.g. delayed afterdepolarizations) may in fact be generated by an increase in Ca^{2+} influx through L-type Ca^{2+} channels in the cardiomyocyte, potentially initiating AF.¹²

Gelsolin is a ubiquitous 82-kD actin-binding protein formed of six homologous subdomains (S1-S6). Activated by Ca^{2+} and acidosis, it changes its conformation exposing actin-binding sites. Active form can sever actin filaments or bind actin monomers preventing its disorganised assembly.

Actin exposed or released by damaged cells activates inflammatory mediators such as LPS (lysophosphatidic acid) and platelet-activating factor enhancing the inflammatory process.¹³

Gelsolin directly binds and inhibits these mediators and its main function is to scavenge proinflammatory actin filaments by severing and capping them,¹⁴ thus counteracting excessive host response to stress. Recombinant gelsolin administration increased survival in experimental sepsis animal models.¹⁵⁻¹⁶ Reduced plasma gelsolin was also observed in patients with rheumatoid arthritis in combination with the presence of gelsolin-actin complexes in the synovial fluid.¹⁷ In the context of POAF, gelsolin could be protective as a guard against an overwhelming inflammatory state.

Furthermore, L-type Ca^{2+} channels are influenced by cytoskeleton structural changes mediated by gelsolin, where its increasing concentration inactivates the channels.¹⁸ Schrickel et al. interestingly described how altered Ca^{2+} currents associated with gelsolin deficiency promote AF in a mouse model.¹⁹ As demonstrated by van Wagoner and colleagues, Ca^{2+} current in atrial myocytes is increased in patients developing POAF generating delayed after depolarisations substrate for AF.¹² Gelsolin deficiency could lead to an increased opening probability of these Ca^{2+} channels leading to increased excitability of the myocardium ultimately promoting AF.

Limitations

There is not enough evidence yet to understand if gelsolin produced in the EAT might act as a paracrine mediator onto the myocardium similarly to other actin binding proteins.²⁰ There is also an obvious problem of sampling EAT at a single point in time. Further studies are needed to understand whether its effects demonstrated on the cardiomyocyte may also be exerted by the epicardial component.

Conclusion

EAT has recently become target of intense research and there is growing evidence of its implication in the genesis and maintenance of AF. We analyse for the first time proteomic changes in the EAT of patients who are predisposed to develop POAF. Several proteins are differentially expressed in the EAT, gelsolin plays an important role in pathways known to be involved in the genesis of POAF such as inflammation and ion channel disturbances. Improving the understanding of the role of EAT may offer novel insights into the prevention and treatment of AF.

Figure legends

Figure 1. A) a representative EAT 2D-DIGE fluorescent image. The proteins expressed in POAF are labelled with Cy5 dye (red spot) and those expressed in SR are labelled with Cy3 dye (green spots). Yellow spots indicate proteins similarly expressed in both groups. B) Corresponding silver-stained gel. The x axis represents the isoelectric point (pI) and the y axis is the molecular weight (Mw) in kilo Daltons (kD). Identified protein spots were labelled with numbers as shown in Table 2.

Figure 2. Western blot validation on EAT protein extracts showing significant gelsolin downregulation in POAF. Anti-gelsolin 1:1000, rabbit polyclonal antibody, ab74420, abcam. Chart based on mean \pm SEM densitometry values. *** = ($p < 0.001$). AU = arbitrary units. SR = sinus rhythm. AF = atrial fibrillation.

Figure 3. Column scatter dot plot graph showing gelsolin gene expression significantly reduced in AF ($p = 0.038$). Values are CT (cycle threshold for gene amplification) fold change against the reference sample. Each dot/square represent one sample value, error bars represent mean with SD.

Table 1: Baseline characteristics of patients in the secretome proteomics group.

Variables	POAF (n=10)	SR (n=10)	p value
Age	69.8 +/-5.7	67.6 +/- 6.4	0.43
Gender (male)	9 (90%)	9 (90%)	1
Hypertension	9 (90%)	7 (70%)	0.58
Diabetes	4 (30%)	3 (40%)	1
EF < 40 %	1	1	1
e-GFR < 60	1 (10%)	2 (20%)	1
Beta blockers pre-op	7 (70%)	7 (70%)	1
Beta blockers post-op	7 (70%)	10 (100%)	0.21
CCS 3-4	0	0	N/A
NYHA III-IV	0	1 (10%)	0.33
Grafts n.	3.3 +/- 0.8	3.4 +/- 0.5	0.75
CPB time	74.4 +/- 31.5	75.4 +/- 14.2	0.93
X-clamp time	44.7 +/- 15.8	48.7 +/- 14.2	0.58

EF = ejection fraction; CCS = Canadian Cardiovascular Society; NYHA = New York Heart Association; CPB = cardiopulmonary bypass; X-clamp = cross clamp. Categorical data are numbers (%); continues data are means \pm SD. p-values for comparisons between patient

Table 2: Human EAT secretome proteins identified by 2D-DIGE and MS/MS (POAF vs. SR).

Spot no.	Protein name	UniProt ID	Theoretical		Number of unique peptides	Number of unique spectra	Number of total spectra	% sequence coverage	Av. Ratio	p Value
			Mw (Da)	pI						
1	Apolipoprotein A-II	APOA2_HUMAN	11,175	6.27	2	3	6	21.00%	-1.66	0.0087
2	Apolipoprotein A-II	APOA2_HUMAN	11,175	6.27	2	3	5	21.00%	-1.24	0.034
3	Transthyretin	TTHY_HUMAN	15,887	5.49	4	6	9	34.00%	-1.4	0.019
4	Coactosin-like protein	COTL1_HUMAN	15,945	5.5	3	3	4	16.90%	-1.32	0.016
4	Transthyretin	TTHY_HUMAN	15,887	5.49	6	7	10	34.70%	-1.32	0.016
5	Ubiquitin-conjugating enzyme E2 N	UBE2N_HUMAN	17,138	6.13	4	5	9	26.30%	-1.57	0.003
5	Transthyretin	TTHY_HUMAN	15,887	5.49	8	9	12	49.70%	-1.57	0.003
6	Transthyretin	TTHY_HUMAN	15,887	5.49	3	5	7	18.40%	-1.53	0.0037
6	Prefoldin subunit 5	PFD5_HUMAN	17,328	5.94	3	3	5	24.70%	-1.53	0.0037
7	Transthyretin	TTHY_HUMAN	15,887	5.49	3	4	6	18.40%	-1.36	0.0051
8	Apolipoprotein A-I	APOA1_HUMAN	30,779	5.56	27	32	51	80.10%	-1.38	0.037
9	Apolipoprotein A-I	APOA1_HUMAN	30,779	5.56	17	22	34	62.50%	-1.28	0.013
10	Apolipoprotein A-I	APOA1_HUMAN	30,779	5.56	12	15	27	40.80%	-1.41	0.019
10	Prelamin-A/C	LMNA_HUMAN	74,141	6.57	15	16	29	17.80%	-1.41	0.019
11	N(G) ₂ N(G)-dimethylarginine	DDAH2_HUMAN	29,644	5.66	12	17	30	55.80%	1.47	0.044

Spot no.	Protein name	UniProt ID	Theoretical		Number of unique peptides	Number of unique spectra	Number of total spectra	% sequence coverage	Av. Ratio	p Value
			Mw (Da)	pI						
dimethylaminohydrolyase 2										
12	Annexin A4	ANXA4_HUMAN	35,884	5.83	10	10	14	32.90%	-1.25	0.046
13	Isochorismatase domain-containing protein 1	ISOC1_HUMAN	32,237	6.96	3	4	7	13.40%	1.47	0.011
14	Actin-related protein 2/3 complex subunit 2	ARPC2_HUMAN	34,334	6.84	4	4	7	12.70%	1.39	0.039
14	Ig gamma-1 chain C region	IGHG1_HUMAN	36,105	8.46	4	5	9	16.40%	1.39	0.039
15	Pigment epithelium-derived factor	PEDF_HUMAN	46,314	5.97	4	4	4	10.30%	-1.24	0.036
15	Prelamin-A/C	LMNA_HUMAN	74,141	6.57	7	7	10	11.40%	-1.24	0.036
15	Vimentin	VIME_HUMAN	53,653	5.05	4	4	6	9.66%	-1.24	0.036
16	Alpha-1-antitrypsin	A1AT_HUMAN	46,738	5.37	8	9	15	20.60%	-1.42	0.024
16	Alpha-2-HS-glycoprotein	FETUA_HUMAN	39,323	5.43	10	14	23	27.80%	-1.42	0.024
17	Alpha-2-HS-glycoprotein	FETUA_HUMAN	39,323	5.43	8	11	19	27.80%	-1.4	0.028
17	Alpha-1-antitrypsin	A1AT_HUMAN	46,738	5.37	8	9	14	18.90%	-1.4	0.028
17	Alpha-1-antichymotrypsin	AACT_HUMAN	47,653	5.33	3	3	5	6.86%	-1.4	0.028
17	Vimentin	VIME_HUMAN	53,653	5.05	15	15	25	31.80%	-1.4	0.028
18	Vitamin D-binding protein	VTDB_HUMAN	52,965	5.4	11	13	24	32.90%	-1.28	0.022
18	Antithrombin-III	ANT3_HUMAN	52,604	6.32	18	23	43	40.90%	-1.28	0.022
19	Antithrombin-III	ANT3_HUMAN	52,604	6.32	15	21	35	37.70%	-1.32	0.012

Spot no.	Protein name	UniProt ID	Theoretical		Number of unique peptides	Number of unique spectra	Number of total spectra	% sequence coverage	Av. Ratio	p Value
			Mw (Da)	pI						
19	60 kDa heat shock protein, mitochondrial	CH60_HUMAN	61,056	5.7	16	18	28	37.20%	-1.32	0.012
19	Vitamin D-binding protein	VTDB_HUMAN	52,965	5.4	9	9	16	28.50%	-1.32	0.012
20	Selenium-binding protein 1	SBP1_HUMAN	52,392	5.93	25	32	56	52.30%	1.3	0.05
21	Selenium-binding protein 1	SBP1_HUMAN	52,392	5.93	26	37	64	54.00%	1.36	0.049
22	Alpha-enolase	ENO4_HUMAN	47,170	7.01	9	9	15	26.50%	-1.3	0.023
23	Prelamin-A/C	LMNA_HUMAN	74,141	6.57	13	14	25	21.80%	-1.42	0.031
24	Beta-2-glycoprotein 1	APOH_HUMAN	38,299	8.34	3	3	4	16.20%	-1.3	0.0025
24	Ig gamma-1 chain C region	IGHG4_HUMAN	35,940	7.18	2	2	3	16.20%	-1.3	0.0025
25	Catalase	CATA_HUMAN	59,757	6.9	16	16	29	32.40%	1.28	0.004
26	Catalase	CATA_HUMAN	59,757	6.9	21	24	35	40.20%	1.23	0.01
27	Gelsolin	GELS_HUMAN	85,698	5.9	19	27	42	34.70%	-1.25	0.042
28	Gelsolin	GELS_HUMAN	85,698	5.9	8	10	17	13.00%	-1.3	0.031
28	Serotransferrin	TRFE_HUMAN	77,064	6.81	7	7	12	12.90%	-1.3	0.031
29	Serotransferrin	TRFE_HUMAN	77,064	6.81	21	23	36	31.10%	-1.27	0.05
30	Serotransferrin	TRFE_HUMAN	77,064	6.81	29	34	58	42.80%	-1.28	0.047
31	Serotransferrin	TRFE_HUMAN	77,064	6.81	39	50	86	52.90%	-1.32	0.028

Spot no.	Protein name	UniProt ID	Theoretical		Number of unique peptides	Number of unique spectra	Number of total spectra	% sequence coverage	Av. Ratio	p Value
			Mw (Da)	pI						
32	Serotransferrin	TRFE_HUMAN	77,064	6.81	31	40	68	47.90%	-1.37	0.023
33	Serotransferrin	TRFE_HUMAN	77,064	6.81	40	51	79	53.30%	-1.31	0.023
34	Serotransferrin	TRFE_HUMAN	77,064	6.81	44	61	109	54.60%	-1.29	0.021
35	Serotransferrin	TRFE_HUMAN	77,064	6.81	52	67	112	67.20%	-1.21	0.042

UniProt ID = protein identifier within Universal Protein Resource (UniProt) knowledgebase; MW = molecular weight; Da = Daltons; pI = isoelectric point; Number of unique peptides = peptides on which protein identification was based; Number of unique spectra = spectra that matched different peptides (even if the peptides overlap) or match 2 different charge states of the same peptide, or match both a peptide and a modified form of the peptide; Number of total spectra = sum of spectra identified in each protein; % sequence coverage = percentage of sequence of the full-length protein covered by the unique peptides that were identified.

Table 3: qPCR delta CT fold change against the reference sample.

SR	ΔcT	POAF	ΔcT
Sample		Sample	
1	1.000	17	0.933
2	3.639	18	1.508
3	2.510	19	0.323
4	2.538	20	1.832
5	3.513	21	1.570
6	0.958	22	2.862
7	1.380	23	1.848
8	3.409	24	2.376
9	2.336		
10	4.474		
11	2.558		
12	4.253		
13	3.625		
14	3.030		
15	0.672		
16	2.899		
	2.675	p value	1.656
		0.0380	

Gene expression for gelsolin shows significant reduction in the POAF group

References

1. Mariscalco G, Klersy C, Zanobini M, Banach M, Ferrarese S, Borsani P, et al. Atrial fibrillation after isolated coronary surgery affects late survival. *Circulation*. 2008;118:1612-8.
2. Kourliouros A, Karastergiou K, Nowell J, Gukop P, Tavakkoli Hosseini M, Valencia O, et al. Protective effect of epicardial adiponectin on atrial fibrillation following cardiac surgery. *European Journal of Cardio-Thoracic Surgery*. 2011;39:228-32.
3. Hatem S, Sanders P. Epicardial adipose tissue and atrial fibrillation. *Cardiovasc Res* 2014;102:205-213.
4. Salgado-Somoza A, Teijeira-Fernandez E, Fernandez AL, Gonzalez-Juanatey JR, Eiras S. Proteomic analysis of epicardial and subcutaneous adipose tissue reveals differences in proteins involved in oxidative stress. *Am J Physiol Heart Circ Physiol* 2010;299:H202-9.
5. Shevchenko A, Wilm M, Vorm O, Mann M. Mass spectrometric sequencing of proteins from silver-stained polyacrylamide gels. *Anal Chem*. 1996;68:850-8.
6. Iwasaki Y, Nishida K, Kato T, Nattel S. Atrial Fibrillation Pathophysiology. *Circulation*. 2011;124:2264-74.
7. Friedrichs K, Klinke A, Baldus S. Inflammatory pathways underlying atrial fibrillation. *Trends Mol Med*. 2011.
8. Mayson SE, Greenspon AJ, Adams S, DeCaro MV, Sheth M, Weitz HH, et al. The changing face of postoperative atrial fibrillation prevention: a review of current medical therapy. *Cardiol Rev*. 2007;15:231.

9. Frustaci A, Chimenti C, Bellocci F, Morgante E, Russo MA, Maseri A. Histological substrate of atrial biopsies in patients with lone atrial fibrillation. *Circulation*. 1997;96:1180-4.
10. Psychari SN, Apostolou TS, Sinos L, Hamodraka E, Liakos G, Kremastinos DT. Relation of elevated C-reactive protein and interleukin-6 levels to left atrial size and duration of episodes in patients with atrial fibrillation. *Am J Cardiol*. 2005;95:764-7.
11. Sata N, Hamada N, Horinouchi T, Amitani S, Yamashita T, Moriyama Y, et al. C-reactive protein and atrial fibrillation. Is inflammation a consequence or a cause of atrial fibrillation? *Jpn Heart J*. 2004;45:441-5.
12. Van Wagoner DR, Pond AL, Lamorgese M, Rossie SS, McCarthy PM, Nerbonne JM. Atrial L-type Ca²⁺ currents and human atrial fibrillation. *Circ Res*. 1999;85:428-36.
13. Osborn TM, Dahlgren C, Hartwig JH, Stossel TP. Modifications of cellular responses to lysophosphatidic acid and platelet-activating factor by plasma gelsolin. *Am J Physiol Cell Physiol*. 2007;292:C1323-30.
14. Lind SE, Smith DB, Janmey PA, Stossel TP. Role of plasma gelsolin and the vitamin D-binding protein in clearing actin from the circulation. *J Clin Invest*. 1986;78:736-42.
15. Christofidou-Solomidou M, Scherpereel A, Solomides CC, Christie JD, Stossel TP, Goelz S, et al. Recombinant plasma gelsolin diminishes the acute inflammatory response to hyperoxia in mice. *J Invest Med*. 2002;50:54-60.
16. Lee PS, Waxman AB, Cotich KL, Chung SW, Perrella MA, Stossel TP. Plasma gelsolin is a marker and therapeutic agent in animal sepsis. *Crit Care Med*. 2007;35:849-55.

17. Osborn TM, Verdrengh M, Stossel TP, Tarkowski A, Bokarewa M. Decreased levels of the gelsolin plasma isoform in patients with rheumatoid arthritis. *Arthritis Res Ther.* 2008;10:R117.
18. Lader AS, Kwiatkowski DJ, Cantiello HF. Role of gelsolin in the actin filament regulation of cardiac L-type calcium channels. *Am J Physiol.* 1999;277:C1277-83.
19. Schrickel JW, Fink K, Meyer R, Grohé C, Stoeckigt F, Tiemann K, et al. Lack of gelsolin promotes perpetuation of atrial fibrillation in the mouse heart. *Journal of interventional cardiac electrophysiology.* 2009;26:3-10.
20. Hinkel R, El-Aouni C, Olson T, Horstkotte J, Mayer S, Muller S, et al. Thymosin beta4 is an essential paracrine factor of embryonic endothelial progenitor cell-mediated cardioprotection. *Circulation.* 2008 Apr 29;117:2232-40.

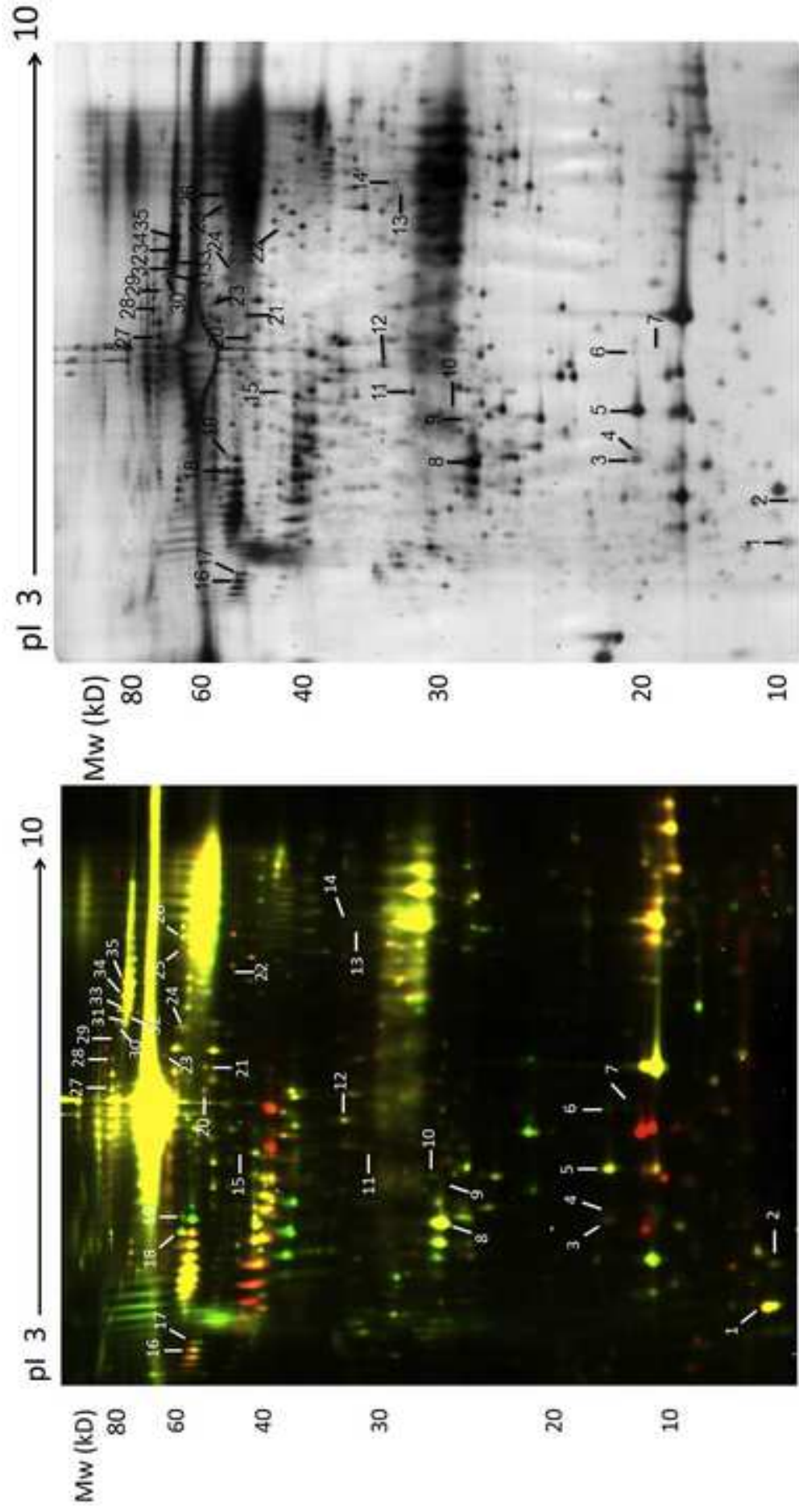
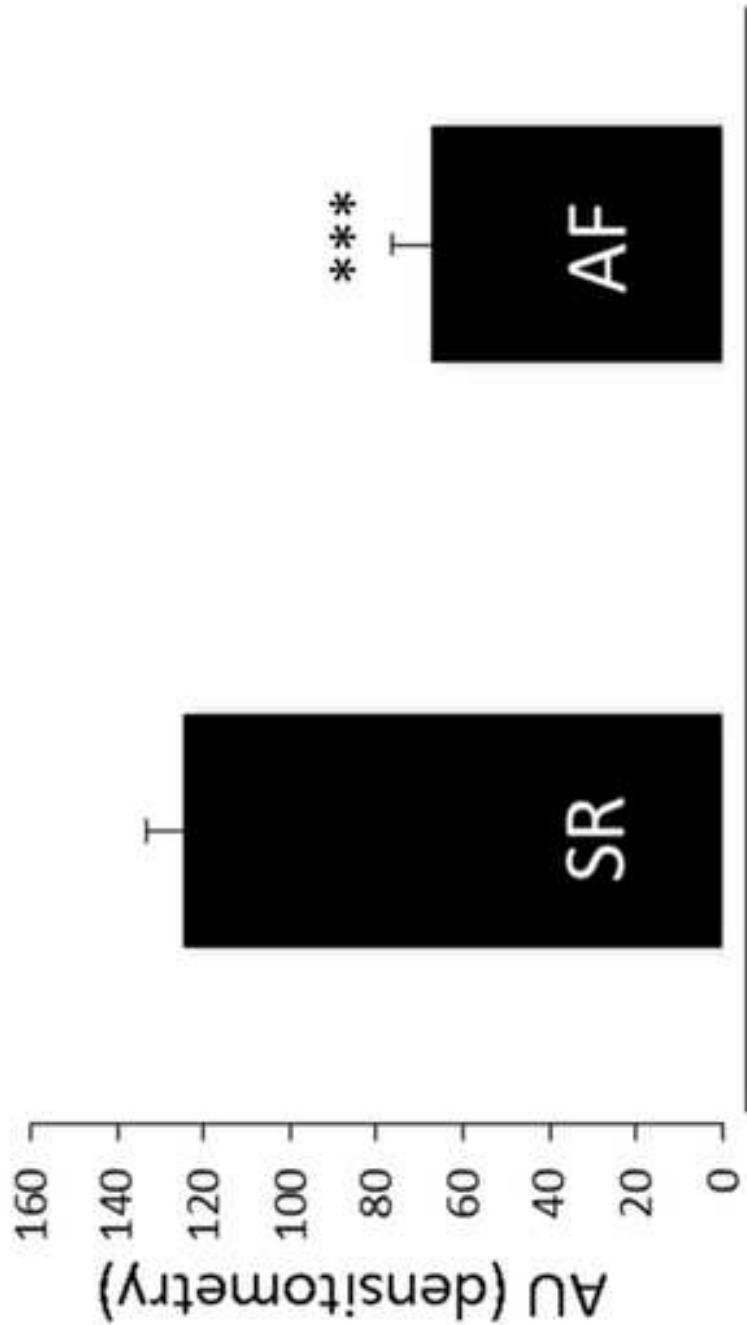
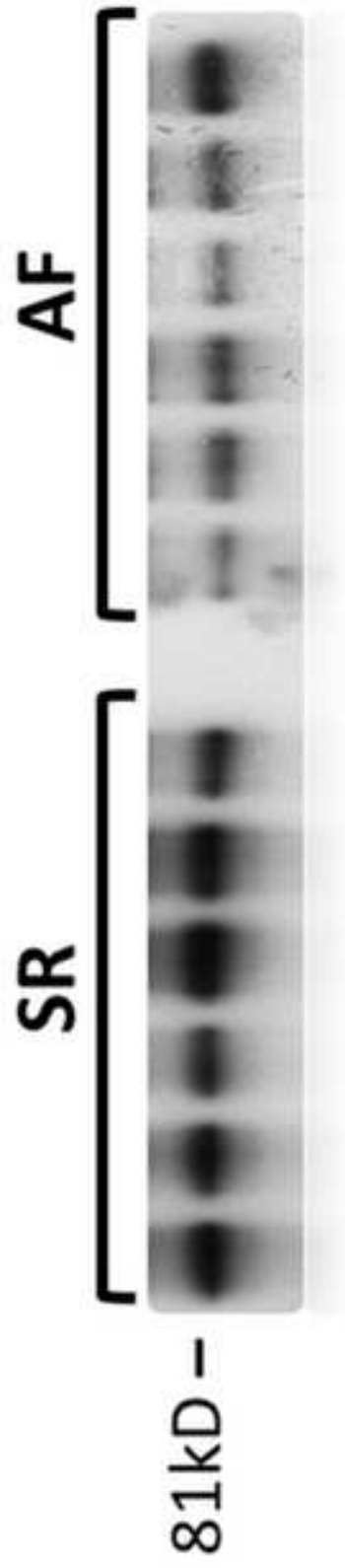
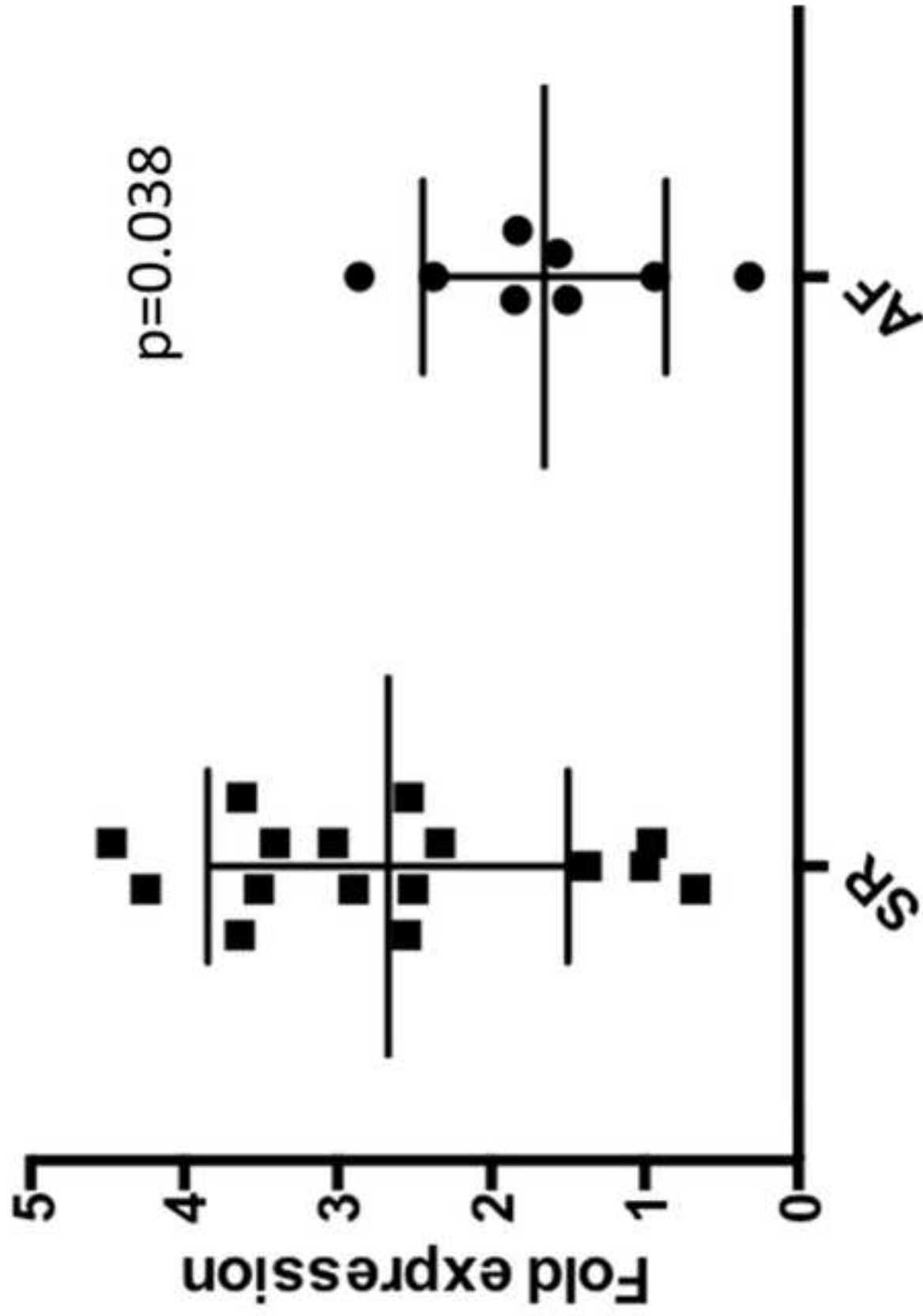


Figure 1



Gelsolin



Page 0

